Gyrofluid investigation of the magnetic field structure associated with edge localised ideal ballooning modes

J. Peer[1], F. Gennrich[1], A. Kendl[1], B.D. Scott[2]

[1] *Institute for Ion Physics and Applied Physics, University of Innsbruck, Association Euratom-ÖAW, A-6020 Innsbruck, Austria*

[2] *Max-Planck-Institute for Plasma Physics, Euratom Association, D-85748 Garching, Germany*

Introduction

The magnetic field structure associated with the linear growth and the nonlinear blowout of pressure driven ideal ballooning modes (IBMs) in the edge pedestal of tokamak H–mode plasmas is investigated numerically within the nonlinear gyrofluid model GEMR.

Gyrofluid model

The gyrofluid model GEMR is based on the formation of moments from the gyrokinetic equation [1]. The moments are density, n_z, parallel and perpendicular temperatures, $T_{z\|}$ and $T_{z\perp}$, and parallel and perpendicular components of the parallel heat flux, $q_{z\|}$ and $q_{z\perp}$, where $z \in \{\mathrm{e}, \mathrm{i}\}$ denotes the species (electrons and ions). The equations are coupled by a polarisation equation involving the electric potential ϕ, and an induction equation yielding the magnetic potential $A_\|$. The full set of model equations is reproduced in refs. [1, 2].

GEMR evolves the gradients in density and temperature as part of the dependent variables, and includes the computation of a time–dependently self–consistent, circular toroidal magnetic equilibrium [3]. The model is based on field aligned coordinates (x, y_k, s), where x is a flux surface label, $y_k = y - \alpha_k$ is a field line label with α_k denoting a shift in order to avoid the deformation of grid cells associated with the magnetic shear, and s denotes the position along the magnetic field [4].

Simulation setup

Since a self consistent simulation of the L–H transition on the basis of the gyrofluid equations is currently not yet possible, the computation of ideal ballooning ELMs requires the artificial preparation of an ideal ballooning unstable ($\alpha_\mathrm{M} = q^2 R \nabla\beta \gtrsim 1$), H–mode like initial state. The initial pedestal profiles are modelled according to experimental values for the ASDEX Upgrade H–mode [5]. The reference values for density, temperature, magnetic flux density, and electron collision time are $n_\mathrm{e} = n_\mathrm{i} = 2.5 \cdot 10^{-19}\,\mathrm{m}^{-3}$, $T_\mathrm{e} = 300\,\mathrm{eV}$, $T_\mathrm{i} = 360\,\mathrm{eV}$, $B = 2\,\mathrm{T}$, and $\tau_\mathrm{e} = 2.56 \cdot 10^{-6}\,\mathrm{s}$, respectively. The initial safety factor profile is prescribed as $q = 1.45 + 3.50 r^2$, where $r =$

ρ/a is the normalised radial coordinate of a toroidal system (ρ, η, ϕ) with $a = 0.5\,\mathrm{m}$ denoting the minor plasma radius. The radial simulation domain has an extension of $0.06\,\mathrm{m}$ around the last closed flux surface located at $r = 1$.

The simulations are started from a turbulent bath of random density fluctuations. A grid resolution of $64 \times 512 \times 16$ points in (x, y_k, s) is used. The time step is set to $0.002\,a/c_\mathrm{s}$, where $c_\mathrm{s} = \sqrt{T_\mathrm{e}/M_\mathrm{i}}$ is the plasma sound speed with M_i denoting the ion mass. During the linear growth phase of the IBM instability, the initially prescribed radial profiles in density and temperature are sustained by appropriate sources. This has been found to be necessary to avoid the formation of ion temperature gradient driven separatrix modes, which usually develop from an unphysical local profile steepening near the separatrix.

Results and discussion

The prepared H–mode state leads to the evolution of an IBM instability with toroidal mode number $n = 6$. If the safety factor profile is modified, instabilities with other toroidal mode numbers can be excited as well. Figure 1 illustrates the temporal evolution in terms of toroidal mode number spectra for the radial magnetic perturbation B^x. The prescribed initial turbulent bath ($t = 1\,a/c_\mathrm{s}$) is characterised by a broad spectrum of randomly distributed magnetic perturbations (fig. 1(a)). During the linear growth phase of the IBM instability ($6\,a/c_\mathrm{s} \lesssim t \lesssim 21\,a/c_\mathrm{s}$), the magnetic perturbations are distributed around the toroidal mode number $n = 6$ (fig. 1(b)). As soon as the instability reaches nonlinear saturation ($21\,a/c_\mathrm{s} \lesssim t \lesssim 25\,a/c_\mathrm{s}$), the spectrum extends radially, which is related to the formation of radially protruding interchange perturbations. Moreover, the lowest harmonics with $n = 12$ and $n = 18$ become excited (fig. 1(c)). The transition to turbulence ($t \gtrsim 25\,a/c_\mathrm{s}$) involves a broadening of the spectrum (fig. 1(d)).

The linear growth phase of the IBM instability is characterised by a pronounced structure in the parallel current (fig. 2(a)). The resulting radial magnetic perturbations (fig. 2(b)) give rise to the formation of magnetic islands. Figure 2(c) shows a Poincaré section for the magnetic field at $t = 14\,a/c_\mathrm{s}$. The considered radial range includes three resonant rational surfaces ($q = 29/6$, $q = 34/7$, $q = 39/8$), which are radially separated by a distance of the order of the drift scale ρ_s. The resonants with $n = 6$ and $n = 7$ are most strongly excited, which is in agreement with fig. 1(b).

Due to several closely located resonant rational surfaces in the radial simulation domain (radial separation of the order of ρ_s), neighbouring chains of magnetic islands start to overlap already during the linear growth phase at $t \approx 17\,a/c_\mathrm{s}$. The resulting magnetic stochasticity is observed to increase until the instability reaches nonlinear saturation. After the IBM blowout, the system passes into an L–mode like, turbulent state, including drift wave and interchange dy-

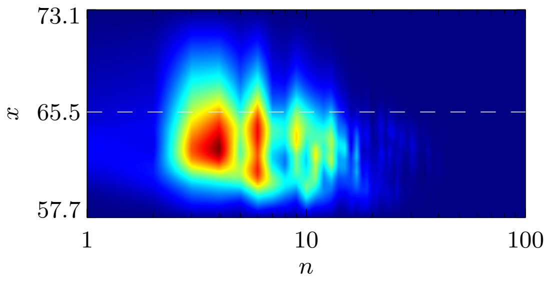

(a) $t = 1\,a/c_s$

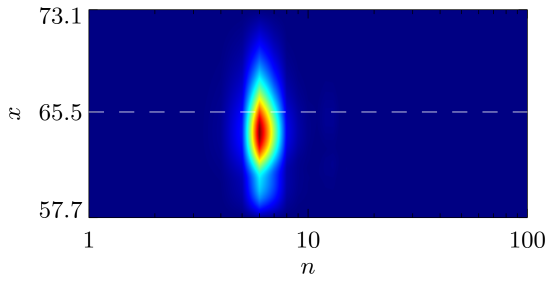

(b) $t = 18\,a/c_s$

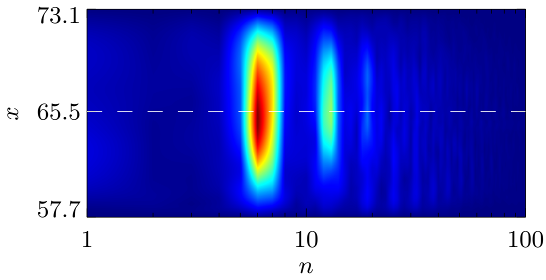

(c) $t = 24\,a/c_s$

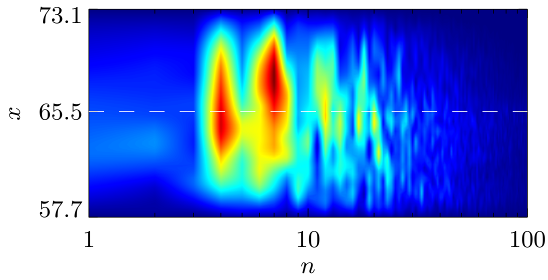

(d) $t = 51\,a/c_s$

Figure 1: Toroidal mode number spectra of the radial magnetic perturbation B^x. The snapshots show the initial turbulent bath (a), the linear growth of the IBM instability (b), the subsequent nonlinear saturation phase (c), and the turbulent aftermath (d). The dashed lines denote the last closed flux surface.

namics. If the turbulence is sustained by L–mode like sources, the magnetic perturbations level off at about 25 % of the maximum perturbations reached during the nonlinear IBM blowout, and the magnetic field remains stochastic. Without any sources, the magnetic stochasticity decreases continuously and the field lines pass into the original equilibrium after about $100\,a/c_s$. Due to the fact that the expected renewed L–H transition after the blowout of the ideal ballooning ELM can not be simulated self–consistently, both scenarios for the turbulent aftermath are of limited validity.

Conclusions and Outlook

The main goal of this study was a detailed analysis of the magnetic field structure associated with an ideal ballooning ELM scenario. The linear growth of edge localised IBM instabilities has been observed to give rise to the formation of rapidly growing chains of magnetic islands, resulting in stochastic magnetic field lines. As a next step, the ideal ballooning ELM scenario will be extended to include the effects of resonant magnetic perturbations.

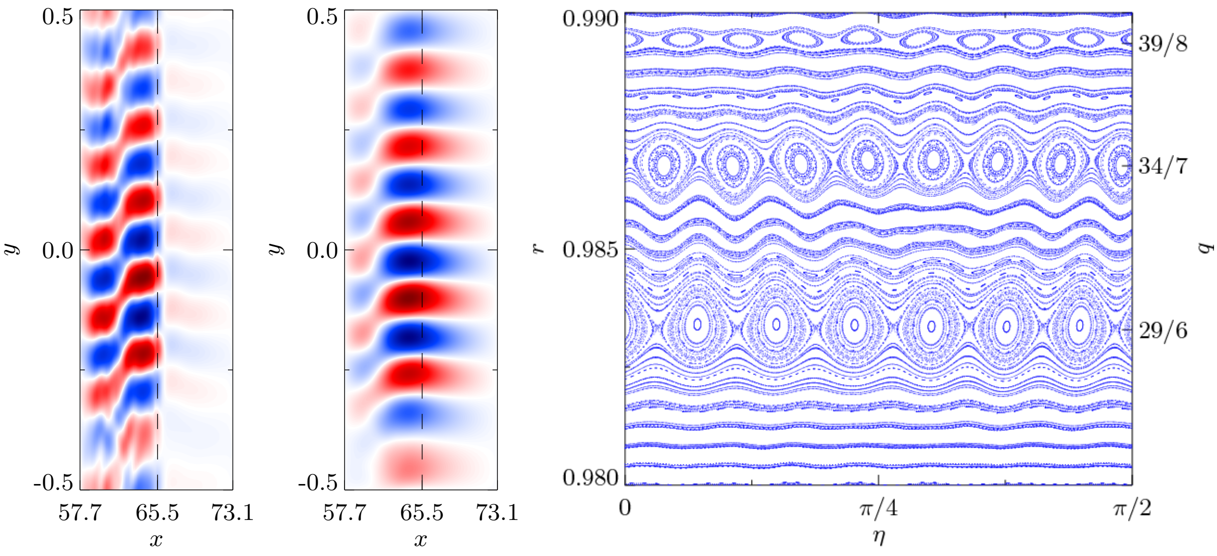

(a) $J_{||}$ (b) B^x (c)

Figure 2: Parallel current (a) and radial magnetic perturbations (b) in the outboard midplane region during the linear growth phase of the IBM instability. The dashed lines denote the last closed flux surface. Figure (c) shows the corresponding Poincaré plot of the magnetic field lines.

Acknowledgements

This work was partly supported by the Austrian Science Fund FWF under Contract No. Y398, by the Austrian Ministry of Science BMWF as part of the UniInfrastrukturprogramm of the Forschungsplattform Scientific Computing at LFU Innsbruck, and by the European Communities under the Contract of Associations between Euratom and the Austrian Academy of Sciences, carried out within the framework of the European Fusion Development Agreement. The views and opinions herein do not necessarily reflect those of the European Commission.

References

[1] B.D. Scott, Phys. Plasmas **12**, 102307 (2005)

[2] A. Kendl et al., Phys. Plasmas **17**, 072302 (2010)

[3] B.D. Scott, Contrib. Plasma Phys. **46**, 714 (2006)

[4] B. Scott, Phys. Plasmas **8**, 447 (2001)

[5] L.D. Horton et al., Nucl. Fusion **45**, 856 (2005)